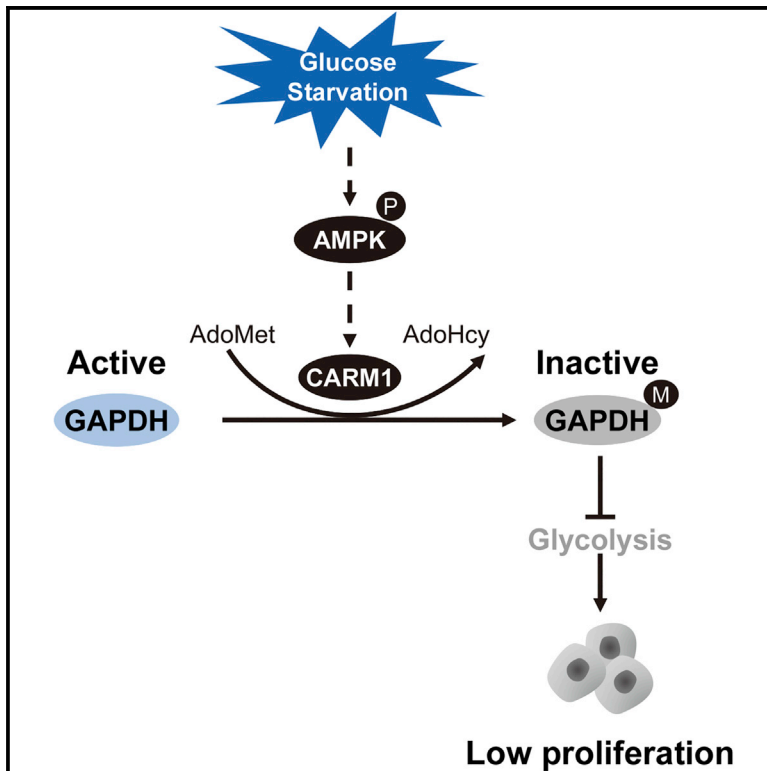


## CARM1 Methylates GAPDH to Regulate Glucose Metabolism and Is Suppressed in Liver Cancer

### Graphical Abstract



### Authors

Xing-Yu Zhong, Xiu-Ming Yuan, Ying-Ying Xu, ..., Hao-Jie Lu, Yi-Ping Wang, Qun-Ying Lei

### Correspondence

yiping\_wang@fudan.edu.cn (Y.-P.W.), qlei@fudan.edu.cn (Q.-Y.L.)

### In Brief

GAPDH is a critical enzyme in glycolysis. Zhong et al. find that CARM1 methylates GAPDH at R234 and inhibits its activity in an AMPK-dependent manner. R234 methylation inhibits glycolysis and proliferation of liver cancer cell lines. In hepatocellular carcinoma patient samples, GAPDH R234 is hypomethylated, and there is a positive correlation between CARM1 levels and R234 methylation.

### Highlights

- CARM1 methylates and inhibits GAPDH in an AMPK-dependent manner
- GAPDH methylation represses glycolysis and proliferation of liver cancer cells
- R234 methylation is positively correlated with CARM1 in hepatocellular carcinoma



# CARM1 Methylates GAPDH to Regulate Glucose Metabolism and Is Suppressed in Liver Cancer

Xing-Yu Zhong,<sup>1</sup> Xiu-Ming Yuan,<sup>1</sup> Ying-Ying Xu,<sup>1</sup> Miao Yin,<sup>2,3</sup> Wei-Wei Yan,<sup>3</sup> Shao-Wu Zou,<sup>4</sup> Li-Ming Wei,<sup>5</sup> Hao-Jie Lu,<sup>5</sup> Yi-Ping Wang,<sup>2,3,\*</sup> and Qun-Ying Lei<sup>2,3,6,7,\*</sup>

<sup>1</sup>Department of Biochemistry and Molecular Biology, School of Basic Medical Sciences, Shanghai Medical College, Fudan University, 131 Dong'an Road, Shanghai 200032, China

<sup>2</sup>Cancer Institute, Fudan University Shanghai Cancer Center and Department of Oncology, Shanghai Medical College, Fudan University, 270 Dong'an Road, Shanghai 200032, China

<sup>3</sup>Cancer Metabolism Laboratory, Institutes of Biomedical Sciences, Shanghai Medical College, Fudan University, 131 Dong'an Road, Shanghai 200032, China

<sup>4</sup>Department of Hepatopancreatobiliary Surgery, Shanghai Tenth People's Hospital, Tong Ji University, 1239 Siping Road, Shanghai 200072, China

<sup>5</sup>Proteomics Center, Institutes of Biomedical Sciences, Shanghai Medical College, Fudan University, 131 Dong'an Road, Shanghai 200032, China

<sup>6</sup>State Key Laboratory of Medical Neurobiology, Fudan University, 131 Dong'an Road, Shanghai 200032, China

<sup>7</sup>Lead Contact

\*Correspondence: [yiping\\_wang@fudan.edu.cn](mailto:yiping_wang@fudan.edu.cn) (Y.-P.W.), [qlei@fudan.edu.cn](mailto:qlei@fudan.edu.cn) (Q.-Y.L.)

<https://doi.org/10.1016/j.celrep.2018.08.066>

## SUMMARY

Increased aerobic glycolysis is a hallmark of cancer metabolism. How cancer cells coordinate glucose metabolism with extracellular glucose levels remains largely unknown. Here, we report that coactivator-associated arginine methyltransferase 1 (CARM1 or PRMT4) signals glucose availability to glyceraldehyde-3-phosphate dehydrogenase (GAPDH) and suppresses glycolysis in liver cancer cells. CARM1 methylates GAPDH at arginine 234 (R234), inhibiting its catalytic activity. Glucose starvation leads to CARM1 upregulation, further inducing R234 hypermethylation and GAPDH inhibition. The re-expression of wild-type GAPDH, but not of its methylation-mimetic mutant, sustains glycolytic levels. CARM1 inhibition increases glycolytic flux and glycolysis. R234 methylation delays tumor cell proliferation *in vitro* and *in vivo*. Compared with normal tissues, R234 is hypomethylated in malignant clinical hepatocellular carcinoma samples. Notably, R234 methylation positively correlates with CARM1 expression in these liver cancer samples. Our findings thus reveal that CARM1-mediated GAPDH methylation is a key regulatory mechanism of glucose metabolism in liver cancer.

## INTRODUCTION

Cancer cells have features that distinguish them from normal cells, including metabolic reprogramming, resistance to cell death, and evasion of growth suppression (Hanahan and Wein-

berg, 2011). Among these features, dysregulated metabolism is regarded as a driving force for tumor initiation and progression (Dang, 2012). Indeed, cancer cells prefer aerobic glycolysis to oxidative phosphorylation even under normoxic conditions, a characteristic known as the Warburg effect (Warburg, 1956). This unique metabolic behavior promotes malignancy by fueling cancer cells' energetic demands and by providing the building blocks for cell proliferation. The activation of glycolytic enzymes is frequently observed in almost all human cancers (Lash et al., 2000; Strausberg et al., 2001). To thrive in a harsh microenvironment, cancer cells coordinate their metabolic program with the availability of extracellular nutrients, especially glucose. However, the mechanism that fine-tunes glucose metabolism and glucose availability within cancer cells remains largely unknown.

Glyceraldehyde-3-phosphate dehydrogenase (GAPDH) is a housekeeping gene that functions in glycolysis. It catalyzes the phosphorylation and oxidation of glyceraldehyde-3-phosphate (G3P), using  $\beta$ -nicotinamide adenine dinucleotide (NAD<sup>+</sup>) as a coenzyme, to produce 1,3-bisphosphoglycerate (1,3-BPG) and NADH (Lehninger et al., 2013). GAPDH plays a vital role in maintaining aerobic glycolysis in various cancers, such as lung cancer, pancreatic adenocarcinoma, and prostate cancer (Ripple and Wilding, 1995; Schek et al., 1988; Tokunaga et al., 1987). However, the mechanism that regulates GAPDH and its effect on glucose utilization remains unclear. The catalytic activity of GAPDH is modulated by levels of extracellular glucose (Li et al., 2014). Upon glucose starvation in HEK293 cells and mouse embryonic fibroblasts (MEFs), GAPDH translocates to the nucleus and enhances autophagy (Chang et al., 2015). These observations strongly suggest that the function of GAPDH is intrinsically linked to nutrient sensing. However, how GAPDH coordinates its catalytic activity with nutrient availability remains obscure.

Protein arginine methylation, catalyzed by protein arginine methyltransferases (PRMTs), is a prevalent post-translational



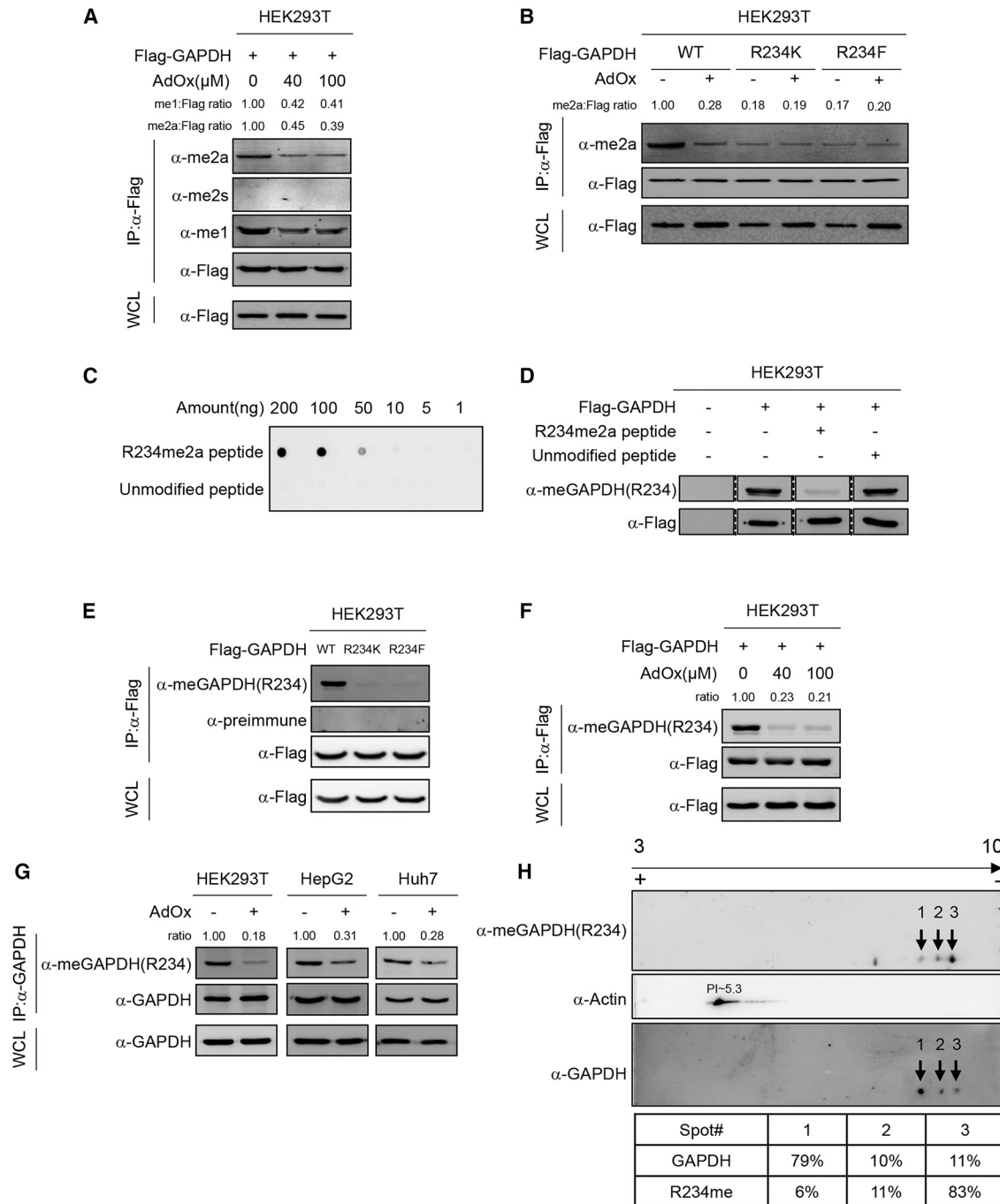


### Figure 1. GAPDH Is Methylated at R234

(A) Arginine methylation of GAPDH is decreased by AdOx treatment. HEK293T cells overexpressing FLAG-tagged GAPDH were treated with increasing concentrations of the PRMT inhibitor AdOx for 24 hr as indicated. Arginine methylation of immunopurified GAPDH was detected with antibodies as indicated. Relative ratios of GAPDH methylation were calculated by normalizing against the GAPDH protein level. WCL, whole-cell lysate.

(B) AdOx decreases arginine methylation of wild-type (WT) GAPDH but not of the R234K and R234F GAPDH mutants. HEK293T cells expressing FLAG-tagged WT GAPDH or the R234K or R234F mutants were treated with or without AdOx for 24 hr. Ectopically expressed GAPDH was affinity-purified using FLAG beads. Arginine methylation of immunopurified GAPDH was analyzed by western blot.

(C) The R234 site-specific methylation antibody  $\alpha$ -meGAPDH(R234) detects the methylated, but not the unmodified, peptide. A nitrocellulose membrane was spotted with different amounts of either R234me2a peptide or unmodified peptide, as indicated, and probed with the  $\alpha$ -meGAPDH(R234) antibody.

(D) The R234me2a peptide, but not the unmodified peptide, blocks the R234 site-specific antibody. The  $\alpha$ -meGAPDH(R234) antibody was incubated with either R234me2a peptide or unmodified peptide for 3 hr at 4°C and used for western blot analysis as indicated. The FLAG antibody was included as a control.

(legend continued on next page)

modification (Paik et al., 2007). The human genome encodes at least nine different PRMTs (Yang and Bedford, 2013). PRMTs catalyze mono- or di-methylation reactions on arginine residues. Because of different catalytic specificities, asymmetric dimethyl-arginine is produced by type I PRMTs (PRMT1, PRMT2, PRMT3, PRMT4, PRMT6, and PRMT8), whereas symmetric Di-methyl-arginine forms with the help of type II PRMTs (PRMT5 and PRMT9) (Bedford and Clarke, 2009; Yang et al., 2015). Protein arginine methylation regulates multiple cellular processes, such as cellular metabolism, transcription, protein translation, and signal transduction (Gao et al., 2015; Hsu et al., 2011; Liao et al., 2015; Liu et al., 2017a; Poornima et al., 2016; Wang et al., 2016; Zhao et al., 2016). The current human and mouse protein methylomes indicate that almost 3% of metabolic enzymes are modified by arginine methylation (Gu et al., 2016; Guo et al., 2014; Larsen et al., 2016; Onwuli et al., 2017). Notably, clinical evidence suggests that PRMTs are deregulated in various cancers (Al-Dhaheeri et al., 2011; Cheung et al., 2007; Frieze et al., 2008; Shia et al., 2012; Yang and Bedford, 2013). These observations imply that PRMTs potentially modulate nutrient sensing and cancer metabolism by regulating the methylation of metabolic enzymes. Here we report that CARM1, also known as PRMT4, mediates the arginine methylation of GAPDH and couples glucose metabolism with nutrient sensing in liver cancer.

## RESULTS

### GAPDH Is Methylated at R234

Previous protein methylome studies have shown that GAPDH is modified by arginine methylation in both mouse and human cells (Guo et al., 2014; Larsen et al., 2016). To examine whether GAPDH is regulated by arginine methylation, FLAG-tagged wild-type (WT) GAPDH was overexpressed in HEK293T cells. Western blot analysis using antibodies against asymmetrical di-methylarginine ( $\alpha$ -me2a), symmetrical di-methylarginine ( $\alpha$ -me2s), and mono-methylarginine ( $\alpha$ -me1) revealed that immunopurified GAPDH undergoes mono-methylation and asymmetrical di-methylation (Figure 1A). This result indicates that GAPDH is indeed arginine-methylated in HEK293T cells. Treatment of these cells with the PRMT inhibitor adenosine-2,3-dialdehyde (AdOx) significantly reduced both the mono-methylation and asymmetrical di-methylation levels of GAPDH, indicating that this enzyme is dynamically modified by arginine methylation. Of note, symmetrical di-methylarginine (me2s) levels were undetectable (Figure 1A), indicating that GAPDH methylation was

potentially modulated by type I PRMT(s) but not by type II PRMT. Previous mass spectrometry studies have reported that arginine 234 (R234) is the only methylated arginine residue in GAPDH (Guo et al., 2014; Larsen et al., 2016). R234 is highly conserved from yeast to humans and is located in the catalytic pocket of GAPDH (Figures S1A and S1B). To investigate whether R234 is the major methylated site in GAPDH, we mutated R234 into either lysine (R234K), a mutation that confers resistance to arginine methylation, or into phenylalanine (R234F), which can mimic methylated arginine. FLAG-tagged WT GAPDH and its mutants were overexpressed in HEK293T cells, followed by treatment with AdOx. Compared with WT GAPDH, the R234K and R234F mutants showed a 5-fold decrease in the basal level of asymmetrical di-methylation (Figure 1B). Importantly, the levels of asymmetrical di-methylation of WT GAPDH were significantly decreased by AdOx treatment, whereas the methylation of R234K and R234F mutants remained unaltered (Figure 1B). This result indicates that R234 is the major, if not the sole, methylation site of GAPDH.

To more precisely monitor the methylation status of GAPDH at R234, we generated a site-specific antibody ( $\alpha$ -meGAPDH(R234)), the specificity of which was validated in both dot blot and peptide competition assays (Figures 1C and 1D). This antibody efficiently reacted with WT GAPDH but not with its R234K and R234F mutants (Figure 1E), further supporting that R234 of GAPDH undergoes methylation. Treating cells with AdOx decreased the methylation of R234 in ectopically expressed GAPDH (Figure 1F). In addition, the methylation of R234 in endogenous GAPDH was significantly reduced by AdOx in HEK293T and in two liver cancer cell lines (HepG2 and Huh7) (Figure 1G). Because arginine methylation modulates the positive charge on the target protein, we performed isoelectric focusing (IEF) to separate unmethylated and methylated GAPDH. Interestingly, GAPDH migrated as three populations (spots 1–3), each of which was recognized by the R234-specific methylation antibody (Figure 1H). The antibody (and, thus, methylation) signal was strongest at spot 3, which corresponded to 11% of total GAPDH protein. These data indicate that at least 11% of GAPDH is methylated on arginine 234. Collectively, R234 of GAPDH is dynamically modified by arginine methylation.

### R234 Methylation Decreases Coenzyme Affinity and Inhibits GAPDH Activity

To explore the effect of R234 methylation on GAPDH, we immunopurified GAPDH from AdOx-treated cells and determined its

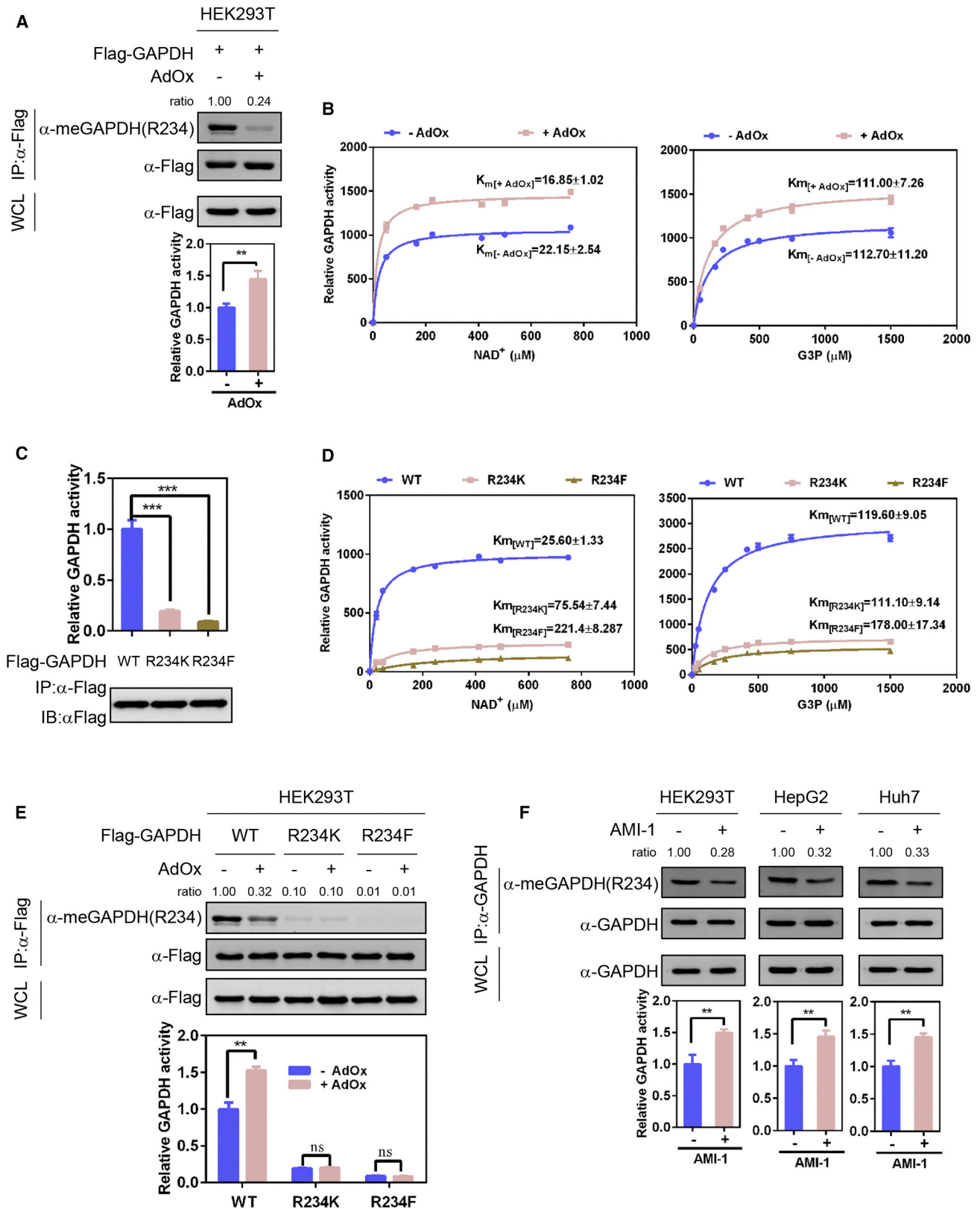
(E) The R234 site-specific methylation antibody recognizes WT GAPDH but not its R234K and R234F mutants. FLAG-tagged WT GAPDH or its R234K and R234F mutants was immunopurified with FLAG beads and blotted with the site-specific methylation antibody  $\alpha$ -meGAPDH(R234) or with serum before immunization. (F and G) AdOx reduces R234 methylation of GAPDH.

(F) HEK293T cells were transfected with FLAG-tagged GAPDH and treated with different concentrations of AdOx. R234 methylation of immunopurified GAPDH was determined using the site-specific antibody  $\alpha$ -meGAPDH(R234).

(G) HEK293T, HepG2, and Huh7 cells were treated with or without AdOx. Endogenous GAPDH was immunoprecipitated using the GAPDH antibody, and R234 methylation was determined by western blot.

(H) Quantitative analysis of endogenous GAPDH methylation at R234. 293T cell lysates were separated by isoelectric focusing (IEF), followed by western blotting using the indicated antibodies. Relative R234 methylation and GAPDH protein levels for each spot were quantified by intensity, and the relative percentage of each spot is calculated and listed below the western blots.

See also Figure S1.



(legend on next page)

catalytic activity. AdOx treatment mediated a significant increase in GAPDH activity concomitant with a decrease in R234 methylation (Figure 2A). We further quantified the catalytic activity of GAPDH on its substrates. AdOx treatment led to a 30% decrease in the  $K_m(\text{NAD}^+)$ , whereas the  $K_m(\text{G3P})$  remained unchanged (Figure 2B). The crystal structure of GAPDH indicates that R234 is located in the catalytic center and that R234 potentially modulates substrate binding; that is, the affinity of GAPDH for G3P and  $\text{NAD}^+$  (Figure S1B; Ismail and Park, 2005; Jenkins and Tanner, 2006). We hypothesized that R234 methylation might inhibit GAPDH activity by regulating the affinity of GAPDH for G3P and/or  $\text{NAD}^+$ . The GAPDH R234K and R234F mutations led to an 80% decrease in GAPDH activity (Figure 2C). Accordingly, the mutation of R234K resulted in a 2-fold increase in  $K_m(\text{NAD}^+)$ , and the R234F mutant showed a 10-fold elevation in  $K_m(\text{NAD}^+)$  (Figure 2D). The  $K_m(\text{G3P})$  of the R234F mutant, but not of the R234K mutant, was elevated by 60% compared with the WT enzyme (Figure 2D). These data show that R234 mutation decreases the affinity of GAPDH for its coenzyme  $\text{NAD}^+$ ; hence, the activity of GAPDH is inhibited. Of note, the R234K mutant of GAPDH showed an unexpected increase in  $K_m(\text{NAD}^+)$  and a decrease in catalytic activity. This observation suggests that R234 is an important residue for catalysis. The R-to-K mutation at R234 strongly disrupted coenzyme binding and suppressed GAPDH activity. R234K is therefore incapable of serving as a methylation-deficient mutant. We nevertheless included the R234K mutant in the functional assays of GAPDH methylation reported below, not to demonstrate its role as a methylation-defective surrogate but to show that GAPDH activity is indispensable for CARM1-mediated glucose sensing and metabolic reprogramming.

We next tested the importance of R234 methylation in controlling GAPDH activity. Cells that express WT GAPDH or its R234K and R234F mutants were treated with AdOx. The activity of the WT enzyme was enhanced by 1.6-fold after AdOx treatment, whereas the activity of the R234K and R234F mutants showed a marginal change in the presence of AdOx (Figure 2E). This result suggests that R234 is a critical site via which arginine methylation regulates the activity of GAPDH. Furthermore, HEK293T, HepG2, and Huh7 cells were treated with arginine

N-methyltransferase inhibitor 1 (AMI-1), a PRMT-specific inhibitor. AMI-1 decreased the R234 methylation of endogenous GAPDH and enhanced its catalytic activity (Figure 2F). Together, these results suggest that R234 methylation inhibits GAPDH by decreasing its affinity for its coenzyme,  $\text{NAD}^+$ .

### CARM1 Methylates GAPDH at R234

The absence of a symmetrical di-methylation signal in GAPDH (Figure 1A) indicates that a type I PRMT, but not a type II PRMT, is responsible for GAPDH methylation. To identify the potential arginine methylase that modifies GAPDH, four different GFP-tagged type I PRMTs (PRMT1–PRMT4) were co-expressed with FLAG-tagged GAPDH. A subsequent co-immunoprecipitation (coIP) assay showed that GAPDH selectively interacted with CARM1 or PRMT4 (Figure 3A). Reciprocal coIP further demonstrated that endogenous CARM1 associated with GAPDH in HEK293T, HepG2, and Huh7 cells (Figures 3B and 3C). To investigate whether CARM1 directly methylates GAPDH, recombinant CARM1 and GAPDH proteins were purified to homogeneity (Figure S2A). A subsequent *in vitro* methylation assay showed that WT CARM1, but not its catalytic-dead R168A mutant, increased R234 methylation and inhibited GAPDH activity (Figure 3D). After incubation with CARM1, GAPDH protein showed an 8-fold increase in  $K_m(\text{NAD}^+)$  and a 1.2-fold increase in  $K_m(\text{G3P})$  (Figure 3E). In contrast, the R234K and R234F mutants showed a negligible change in R234 methylation,  $K_m(\text{NAD}^+)$ ,  $K_m(\text{G3P})$ , or enzyme activity following *in vitro* methylation (Figures 3F and 3G). Collectively, these results strongly support that CARM1 is a direct methylase of GAPDH. CARM1-mediated R234 methylation decreases GAPDH's affinity for  $\text{NAD}^+$  and downregulates GAPDH enzymatic activity.

To test the effect of CARM1 on GAPDH in cells, GAPDH and CARM1 were co-transfected into HEK293T cells. Co-expression of CARM1 with GAPDH increased R234 methylation in a dose-dependent manner, with a corresponding decrease in its activity (Figure S2B). The R168A mutant of CARM1 failed to upregulate R234 methylation and could not suppress GAPDH activity (Figure S2C). More importantly, inhibition of CARM1 by a specific inhibitor, TP-064, or via short hairpin RNA (shRNA) resulted in a strong reduction of R234 methylation in multiple cell lines

### Figure 2. R234 Methylation Decreases Coenzyme Affinity and Inhibits GAPDH Activity

(A) R234 methylation inhibits GAPDH activity. HEK293T cells expressing FLAG-tagged GAPDH were treated with AdOx for 24 hr. GAPDH protein was immunopurified with FLAG beads and eluted with FLAG peptide. GAPDH protein and R234 methylation were determined by western blot. The enzymatic activity of GAPDH was assayed and normalized to GAPDH protein. Relative enzymatic activity is presented as mean  $\pm$  SD of triplicate experiments and was statistically analyzed using unpaired Student's t test. \*\* $p < 0.01$ .

(B) R234 methylation of GAPDH increases its  $K_m(\text{NAD}^+)$  but not  $K_m(\text{G3P})$ . The  $K_m(\text{NAD}^+)$  and  $K_m(\text{G3P})$  of GAPDH immunopurified from cells treated with or without AdOx were determined. Relative enzymatic activity was presented as mean  $\pm$  SD of triplicate experiments.

(C and D) R234K and R234F mutations inhibit the catalytic activity of GAPDH and increase  $K_m(\text{NAD}^+)$ . FLAG-tagged WT GAPDH and its R234K and R234F mutants were immunopurified from HEK293 cells. The catalytic activity of GAPDH (C) and its  $K_m$  for substrates (D) were determined. Relative enzymatic activity was presented as mean  $\pm$  SD of triplicate experiments and was statistically analyzed using unpaired Student's t test. \*\*\* $p < 0.001$ .

(E) AdOx treatment upregulates the activity of WT GAPDH, but not of its R234K and R234F mutants. HEK293T cells expressing FLAG-tagged WT GAPDH or its mutants were treated with or without AdOx for 24 hr. GAPDH protein was immunopurified using FLAG beads and eluted with FLAG peptide. The R234 methylation level and activity of GAPDH were determined. Relative enzymatic activity was presented as mean  $\pm$  SD of triplicate experiments and was statistically analyzed using unpaired Student's t test. \*\* $p < 0.01$ ; ns, not significant.

(F) AMI-1 treatment decreases R234 methylation of endogenous GAPDH and increases its catalytic activity. HEK293T, HepG2, and Huh7 cells were treated with or without the PRMT inhibitor AMI-1. Endogenous GAPDH was immunopurified by using the GAPDH antibody. The R234 methylation and enzyme activity of GAPDH were determined. Relative enzymatic activity was presented as mean  $\pm$  SD of triplicate experiments and was statistically analyzed using unpaired Student's t test. \*\* $p < 0.01$ .

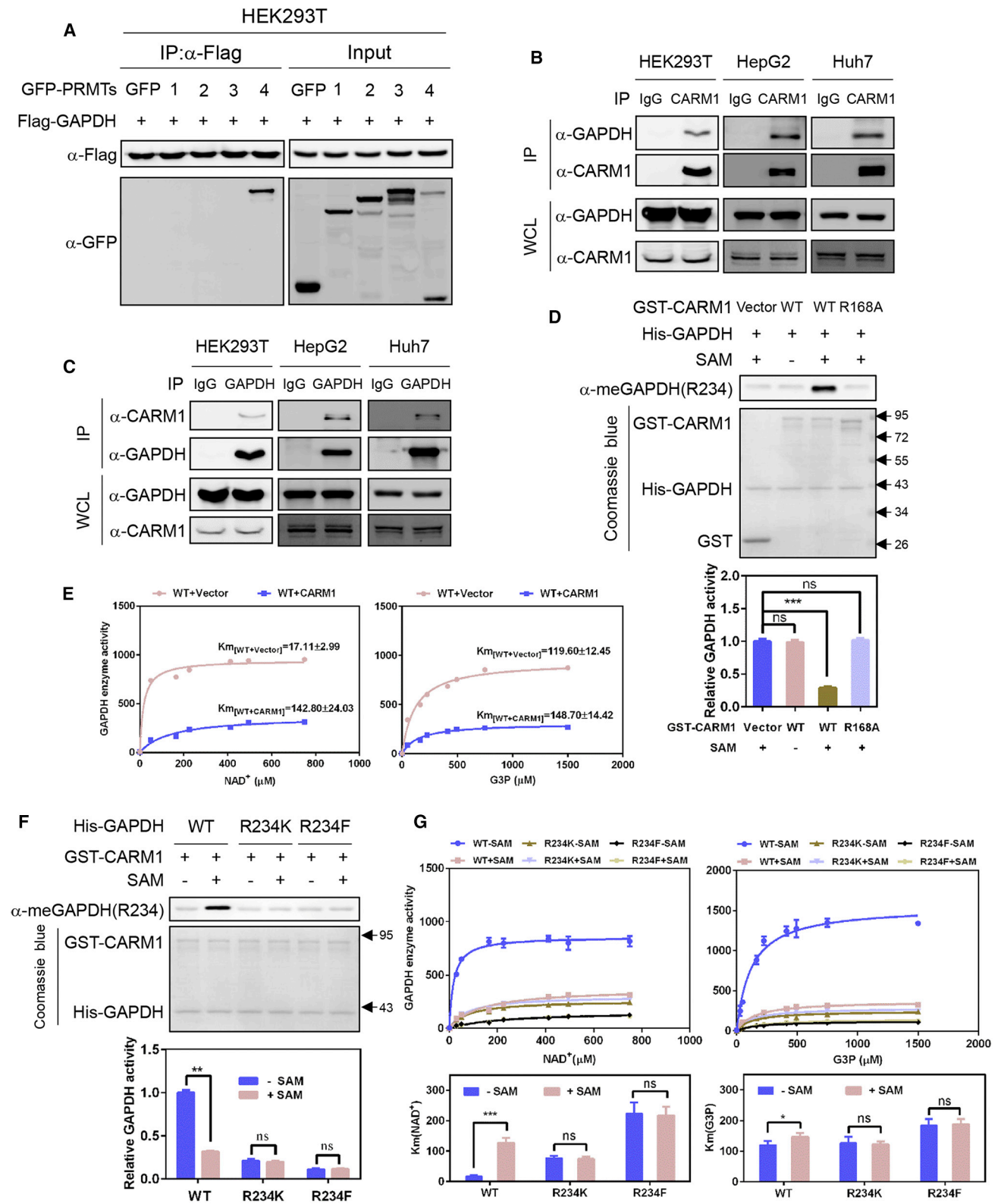


**Figure 3. CARM1 Methylates GAPDH at R234**

(A) GAPDH selectively binds to CARM1 or PRMT4. FLAG-tagged GAPDH was co-expressed with GFP-tagged PRMT1–PRMT4. The GFP-only vector was included as a negative control. GAPDH was immunopurified with FLAG beads. The interaction between GAPDH and PRMT was determined by western blot.

(legend continued on next page)

(HEK293T, HepG2, and Huh7) and in a concomitant increase in the activity of GAPDH (Figures S2D and S2E). Together, these findings show that CARM1 methylates GAPDH at R234 and inhibits its enzymatic activity.

### CARM1 Signals Glucose Availability to GAPDH Methylation in an AMPK-Dependent Manner

The activity of GAPDH is closely linked with glucose availability. We speculated that GAPDH might couple glucose metabolism to extracellular glucose levels. Interestingly, glucose starvation increased the protein expression of CARM1 in HepG2 and Huh7 cells (Figure 4A). The methylation of R234 in GAPDH was also upregulated by glucose depletion in a time-dependent manner, with a corresponding decrease in GAPDH activity (Figure 4A). Previous studies have suggested that glucose starvation induces the phosphorylation of serine 122 (S122) of GAPDH and promotes the nuclear translocation of GAPDH to enhance autophagy (Chang et al., 2015). In line with this finding, we observed an increase in GAPDH phosphorylation upon glucose starvation (Figure 4A). Interestingly, the subcellular localization of WT GAPDH remained unchanged in HEK293T and Huh7 cells treated with TP-064 (Figures S3A and S3B), as did that of the R234K and R234F mutants (Figure S3A). In glucose-starved cells, phosphorylation of the WT GAPDH protein and its R234K mutant was increased, whereas the phosphorylation-resistant S122A mutant showed increased R234 methylation (Figure 4B). In contrast to the S122A mutant, WT GAPDH and its R234K mutant retained the ability to upregulate LC3B, an autophagy marker, under conditions of glucose starvation (Figure 4B). These observations suggest that R234 methylation modulates GAPDH in a manner that is independent of GAPDH phosphorylation. More importantly, CARM1 expression was reduced in a dose-dependent manner when cells were cultured with increasing concentrations of glucose (Figure 4C). In support of this finding, R234 methylation was concomitantly downregulated, and the catalytic activity of GAPDH was upregulated (Figure 4C). These results demonstrate that R234 methylation does not regulate GAPDH localization, nor does it correlate with S122 phosphorylation. Glucose insufficiency increases CARM1 expression, leading to R234 hypermethylation and to inhibition

of GAPDH. Thus, CARM1 links glucose availability to GAPDH activity.

Next, we investigated the underlying mechanism that links glucose levels and R234 methylation. In HepG2 and Huh7 cells, glucose shortage induced the upregulation of the CARM1 protein but not of its mRNA (Figures 4A–4C, S3C, and S3D). AMPK is a multi-subunit kinase complex that senses glucose availability (Hardie, 2014). The alpha subunit of AMPK, designated AMPK $\alpha$ , functions as the catalytic subunit of the AMPK complex. The phosphorylation of AMPK $\alpha$  closely reflects glucose availability and modulates glucose sensing or signaling (Garcia and Shaw, 2017). Notably, the glucose starvation-mediated phosphorylation of AMPK $\alpha$  positively correlated with CARM1 protein expression (Figures 4A–4C), indicating that CARM1 might be involved in glucose signaling in an AMPK-dependent manner. To test whether AMPK modulates CARM1-mediated GAPDH methylation, we employed AMPK $\alpha$  double knockout (DKO) cells, in which two genes (AMPK $\alpha$ 1 or AMPK $\alpha$ 2) that encode the AMPK complex alpha subunits were deleted. In contrast to WT cells, AMPK $\alpha$ -deleted 293A and MEF cells showed no change in CARM1 protein expression or R234 methylation upon glucose starvation (Figures 4D). Glucose starvation also did not alter CARM1 mRNA levels (Figure S3E) in AMPK $\alpha$ -deleted 293A and MEF cells, suggesting that AMPK regulates CARM1 expression post-translationally. A previous study has suggested that CARM1 protein is under the control of the ubiquitin-proteasome pathway (Shin et al., 2016). To investigate this possibility, we treated glucose-starved HepG2 and Huh7 cells with MG132, a proteasome inhibitor. MG132 treatment led to an increase in CARM1 protein; however, glucose starving of cells in the presence of MG132 did not further elevate CARM1 protein levels (Figure S3F). These observations suggest that, in response to glucose availability, AMPK modulates GAPDH methylation by regulating CARM1 protein levels. In addition, in HepG2 and Huh7 cells, shRNA-induced depletion of CARM1 had no effect on AMPK $\alpha$  phosphorylation (Figure 4E). Glucose starvation thus increased R234 methylation and reduced GAPDH activity in control cells but not in CARM1 knockdown cells (Figure 4E). Together, these results show that CARM1 acts in concert with AMPK to signal glucose availability to GAPDH.

(B and C) Endogenous CARM1 associates with GAPDH. Endogenous CARM1 was immunoprecipitated from HEK293T, HepG2, and Huh7 cells with the CARM1 antibody. IgG was included as a negative control (B). Reciprocal coIP was performed using the GAPDH antibody (C). The interaction of endogenous CARM1 and GAPDH was determined by western blot.

(D) WT CARM1 but not its catalytically dead R168A mutant methylates GAPDH *in vitro*. Recombinant CARM1 and GAPDH were incubated with or without S-adenosyl methionine (SAM). GST only was used as a negative control. After *in vitro* methylation, the reaction mixture was subjected to R234 methylation detection, Coomassie blue staining, and a GAPDH enzyme activity assay. Relative enzymatic activity was presented as mean  $\pm$  SD of triplicate experiments and was statistically analyzed using unpaired Student's t test. \*\*\*p < 0.001.

(E) CARM1-catalyzed *in vitro* R234 methylation increases Km(NAD<sup>+</sup>) and Km(G3P) of GAPDH. The *in vitro* methylation assay was performed by incubating GAPDH with GST or with CARM1. Km(NAD<sup>+</sup>) and Km(G3P) of unmethylated and *in vitro*-methylated GAPDH were determined. Relative enzymatic activity was presented as mean  $\pm$  SD of triplicate experiments.

(F) CARM1 increases R234 methylation and decreases the enzymatic activity of WT GAPDH but not of its R234K and R234F mutants *in vitro*. WT GAPDH or its R234K/F mutants was incubated with recombinant CARM1 in the presence or absence of SAM. R234 methylation and the enzymatic activity of GAPDH were determined. Relative enzymatic activity was presented as mean  $\pm$  SD of triplicate experiments and was statistically analyzed using unpaired Student's t test. \*\*p < 0.01.

(G) CARM1 increases Km(NAD<sup>+</sup>) of WT GAPDH but not of its R234K/F mutants *in vitro*. Recombinant GAPDH or its R234K/F mutants were incubated with CARM1 in the presence or absence of SAM. Km(NAD<sup>+</sup>) and Km(G3P) of *in vitro*-methylated GAPDH were determined. Km value was presented as mean  $\pm$  SD of triplicate experiments and was statistically analyzed using unpaired Student's t test. \*\*\*\*p < 0.001, \*p < 0.05.

See also Figure S2.

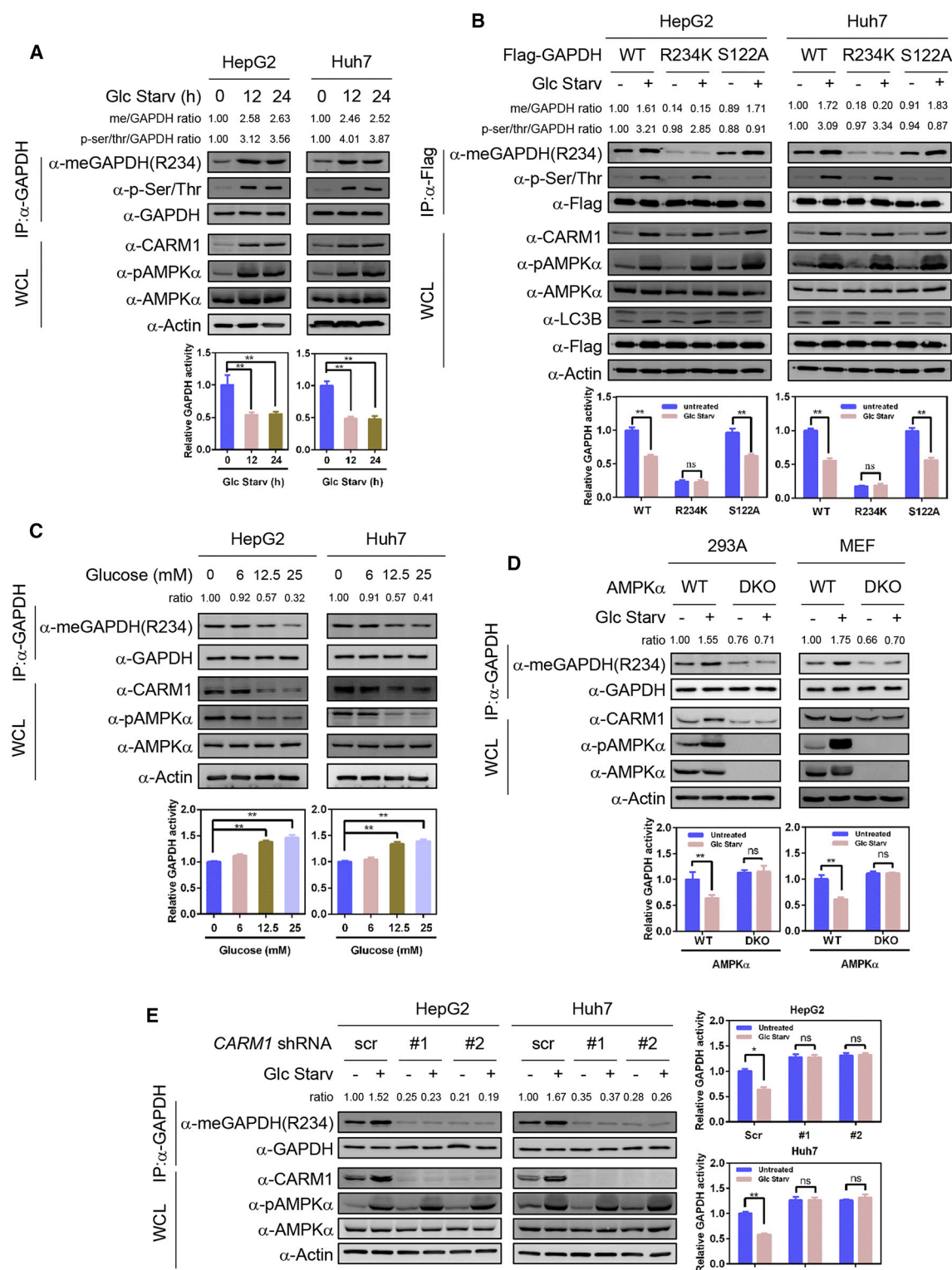


**Figure 4. CARM1 Signals Glucose Availability to GAPDH Methylation in an AMPK-Dependent Manner**

(A) Glucose starvation upregulates GAPDH methylation and decreases GAPDH activity in a time-dependent manner. HepG2 and Huh7 cells were exposed to glucose starvation (Glc Starv) as indicated. Phosphorylation, R234 methylation, and the catalytic activity of immunopurified endogenous GAPDH were determined. The phosphorylation level of AMPK $\alpha$  and CARM1 protein expression were analyzed by western blot. Relative enzymatic activity was presented as mean  $\pm$  SD of triplicate experiments and was statistically analyzed using unpaired Student's t test.

(legend continued on next page)

### GAPDH R234 Methylation Represses Glycolysis

GAPDH plays a critical role in glycolysis. We hypothesized that the R234 methylation of GAPDH potentially represses glycolysis. To test this, we transduced liver cancer cells with shRNA to knock down *GAPDH* and re-introduced WT GAPDH or its R234K and R234F mutants at physiologically relevant levels (Figure S4A). Depletion of *GAPDH* resulted in a significant decrease in glucose consumption and lactate production in both HepG2 and Huh7 cells (Figures S4B and S4C). Re-introducing WT GAPDH restored glucose consumption and lactate secretion but not when the R234F mutant protein was introduced (Figures S4B and S4C). These data indicate that the methylation-mimic mutant R234F suppresses glycolysis in liver cancer cells.

To determine the function of R234 methylation in modulating glycolysis, we re-expressed WT GAPDH or its R234F mutant in *GAPDH* knockdown or *GAPDH/CARM1* double knockdown HepG2 cells (Figures 5A and 5B). Suppression of CARM1 in these cells with TP-064 or via shRNA led to a significant decrease in R234 methylation and to a marked and significant increase in the enzymatic activity of WT GAPDH but not of its R234F mutant (Figures 5C and 5D). Accordingly, the levels of metabolites that lie upstream of GAPDH, including of glucose-6-phosphate (G6P) and G3P, significantly decreased upon CARM1 inhibition. The levels of downstream metabolites, such as 3-phosphoglycerate (3PG), pyruvate, and lactate, significantly increased upon CARM1 inhibition (Figures 5E and 5F). CARM1 inhibition had no effect on the levels of glycolytic metabolites in HepG2 cells in which the R234F mutant was re-expressed (Figures 5E and 5F). We also investigated the effect of GAPDH methylation on glycolysis by suppressing CARM1 with TP-064 or via shRNA in HepG2 cells. The suppression of CARM1 using both approaches significantly upregulated the extracellular acidification rate (ECAR) of cells in which WT GAPDH, but not its R234F mutant, was re-expressed (Figures 5G and 5H). Interestingly, CARM1 inhibition mildly increased the basal oxygen consumption rate (OCR) of cells re-expressing WT GAPDH but not its R234F mutant (Figures 5I and 5J). Collectively, these results suggest that the R234 methylation of GAPDH slows down glycolysis.

### GAPDH R234 Methylation Delays Liver Cancer Cell Growth

Cancer cells depend on enhanced glycolysis to maintain their rapid proliferation. We hypothesized that R234 methylation of GAPDH suppresses cell proliferation. In support of this theory, knockdown of *GAPDH* significantly delayed the proliferation of both HepG2 and Huh7 cells (Figures S5A and S5B). The re-expression of WT GAPDH, but not of its R234F mutant, restored cell growth to a level comparable with scramble shRNA control cells (Figures S5A and S5B). These results indicate that the methylation-mimetic R234F mutant suppresses the proliferation of HepG2 and Huh7 cells.

To further investigate the role of R234 methylation in cell proliferation, *CARM1* was depleted from *GAPDH* knockdown or *GAPDH/CARM1* double knockdown HepG2 cells in which WT GAPDH or its R234F mutant were then re-expressed (Figures 5A and 5B). CARM1 suppression by TP-064 or via shRNA-mediated knockdown significantly promoted the proliferation of cells rescued by WT GAPDH but not that of cells re-expressing the R234F mutant (Figures 6A and 6B). More importantly, CARM1 depletion accelerated the growth of xenograft tumors generated from *GAPDH/CARM1* double knockdown HepG2 cells that re-expressed WT GAPDH but not its R234F mutant (Figures 6C–6E). In addition, we found Ki67 staining to be stronger in tumor xenograft cells in which WT GAPDH was re-expressed relative to R234F-rescued tumor cells (Figure 6F). Moreover, *CARM1* depletion in HepG2 cells re-expressing WT GAPDH led to an increase in 3PG, pyruvate, and lactate levels and to a decrease in G6P and G3P, but not in cells re-expressing the R234F mutant (Figure 6G). These findings were further supported by the sustained re-expression of GAPDH in xenograft tumors in which *CARM1* was stably knocked down (Figure 6H). Together, these results strongly suggest that the methylation of R234 in GAPDH inhibits cell proliferation.

### GAPDH R234 Is Hypomethylated in Human Hepatocellular Carcinoma

To investigate the clinical relevance of GAPDH methylation, we collected 20 samples of human hepatocellular carcinoma (HCC) with paired surrounding normal liver tissue. Immunoblotting of

(B) Glucose starvation inhibits the enzymatic activity of both WT GAPDH and its S122A mutant but not its R234K mutant. *GAPDH* knockdown HepG2 and Huh7 cells re-expressing FLAG-tagged WT GAPDH or its R234K and S122A mutant were cultured with or without glucose for 18 hr. Phosphorylation and R234 methylation of GAPDH and LC3B were determined by western blot. GAPDH activity was analyzed by spectrofluorometer. Relative enzymatic activity was presented as mean  $\pm$  SD of triplicate experiments and was statistically analyzed using unpaired Student's t test.

(C) High glucose induces R234 hypomethylation and GAPDH activation. HepG2 and Huh7 cells were cultured for 18 hr with different concentrations of glucose as indicated. R234 methylation and the catalytic activity of immunopurified endogenous GAPDH were determined. The phosphorylation level of AMPK $\alpha$  and CARM1 protein expression were analyzed by western blot. Relative enzymatic activity was presented as mean  $\pm$  SD of triplicate experiments and was statistically analyzed using unpaired Student's t test.

(D) Glucose starvation-induced R234 hypermethylation is dependent on AMPK $\alpha$ . *AMPK $\alpha$ 1* and *AMPK $\alpha$ 2* double knockout cells (*AMPK $\alpha$*  DKO) or WT cells were cultured with or without glucose for 18 hr. R234 methylation and enzymatic activity of immunoprecipitated GAPDH were assayed. Phosphorylation of AMPK $\alpha$  and protein expression of CARM1 were determined by western blot. Relative enzymatic activity was presented as mean  $\pm$  SD of triplicate experiments and was statistically analyzed using unpaired Student's t test.

(E) Glucose starvation modulates GAPDH methylation in a CARM1-dependent manner. A control shRNA (scr) or two different shRNAs (#1 and #2) targeting *CARM1* were transduced into HepG2 and Huh7 cells. The cells were cultured with or without glucose for 18 hr. The levels of GAPDH R234 methylation, AMPK $\alpha$  phosphorylation, and CARM1 protein expression were analyzed by western blot. The catalytic activity of immunopurified endogenous GAPDH was also determined by spectrofluorometer. Relative enzymatic activity was presented as mean  $\pm$  SD of triplicate experiments and was statistically analyzed using unpaired Student's t test.

\*\*p < 0.01., \*\*p < 0.01. See also Figure S3.

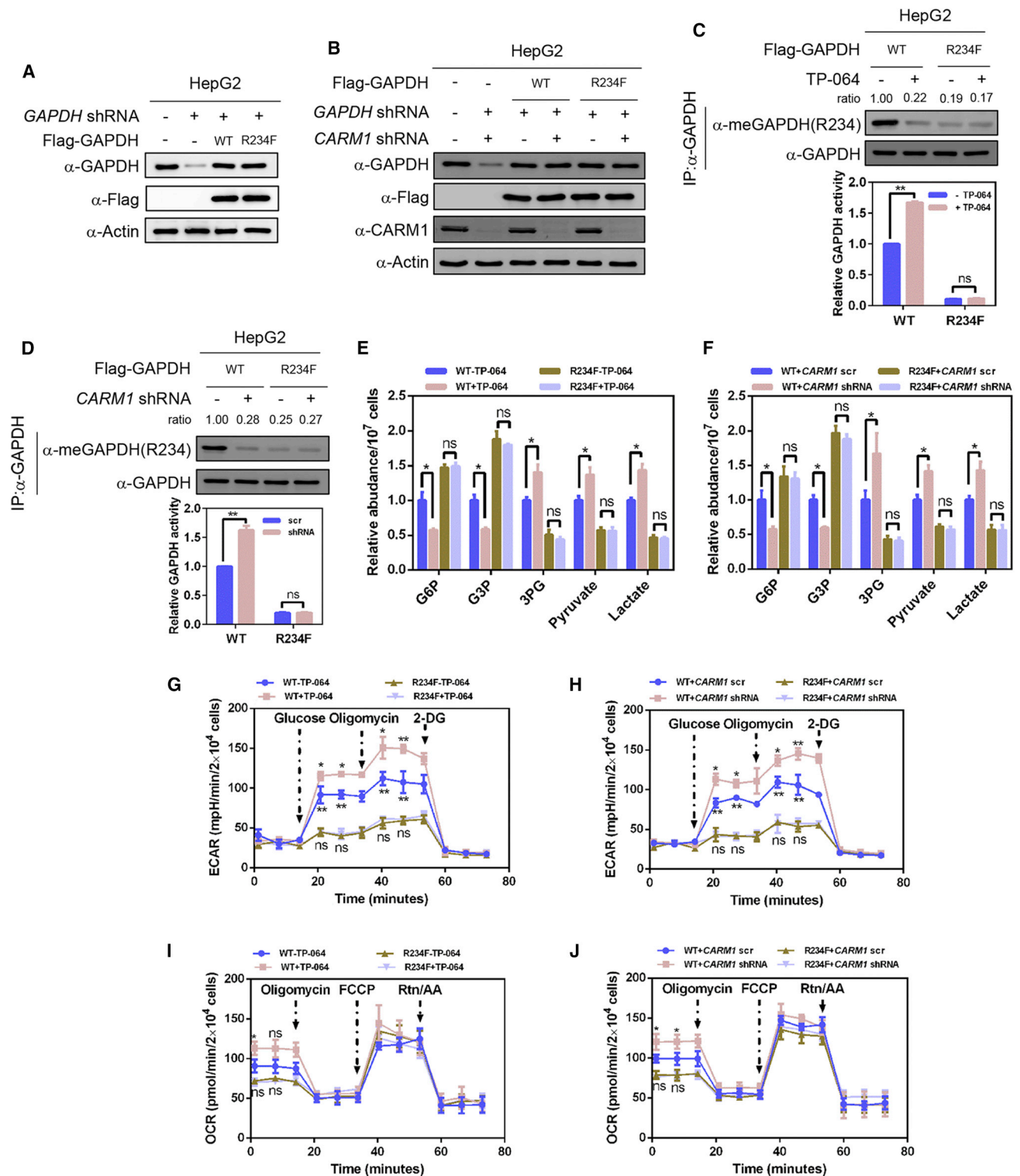


**Figure 5. GAPDH R234 Methylation Represses Glycolysis**

(A and B) Stable re-expression of GAPDH in HepG2 cells. WT GAPDH and its R234F mutant were re-introduced in GAPDH knockdown cells (A) or into GAPDH/CARM1 double knockdown cells (B). Knockdown efficiency and re-expression of FLAG-tagged GAPDH were determined by western blot.

(C and D) TP-064 treatment or CARM1 shRNA decreases R234 methylation and increases the enzymatic activity of WT GAPDH but not of its R234F mutant. GAPDH knockdown HepG2 cells re-expressing WT GAPDH or its R234F mutant were treated with TP-064 (C) or transduced with a virus carrying CARM1 shRNA

(legend continued on next page)

the HCC liver cancer samples (T) and their adjacent normal tissues (N) demonstrated that CARM1 protein levels and R234 methylation levels were significantly lower in the liver cancer tissue ( $p = 0.0001$  and  $p = 0.0007$ ) relative to the surrounding normal tissue (Figures 7A–7D). Moreover, the levels of CARM1 protein expression and R234 methylation positively correlated ( $R2 = 0.626$ ,  $p < 0.0001$ ) (Figure 7E). These data demonstrate that GAPDH methylation is dependent on CARM1 and is involved in the aerobic glycolysis of HCC.

## DISCUSSION

The GAPDH enzyme plays a critical role in the aerobic breakdown of glucose (Lehninger et al., 2013). GAPDH expression is frequently elevated in various human cancers and is associated with reduced patient survival (Lash et al., 2000; Liu et al., 2017b; Strausberg et al., 2001), indicating that GAPDH is involved in metabolic remodeling in a range of different cancers. In this study, we have discovered that GAPDH is regulated by R234 methylation. The CARM1-mediated R234 methylation of GAPDH inhibits its catalytic activity and suppresses the proliferation of liver cancer cells *in vitro* and *in vivo*. More importantly, CARM1 signals glucose availability to GAPDH in an AMPK-dependent manner and coordinates glycolytic activity with extracellular glucose levels (Figure 7F). This finding reveals a new mechanism for how cancer cells couple remodeled metabolism with nutrient sensing.

Methylation of GAPDH at R234 is dynamically regulated, indicating that an arginine demethylase likely modifies this residue. To date, several  $\alpha$ -ketoglutarate ( $\alpha$ -KG)-dependent dioxygenases have been reported to possibly function as arginine demethylases (Walport et al., 2016). However, the methylation of R234 showed only marginal changes when GAPDH was co-expressed with these potential demethylases (data not shown). Thus, the demethylase of GAPDH remains to be discovered.

R234 of GAPDH serves as a key residue during catalysis. Interestingly, it has been reported that the 2,3-butanedione modification of rabbit GAPDH at arginine 231, which corresponds to R234 in human GAPDH, disrupts the enzyme's activity (Kuzminskaya et al., 1991). Although R234 is located in the catalytic center of GAPDH, the enzyme's crystal structure suggests that R234 does not directly interact with  $\text{NAD}^+$  (Jenkins and Tanner, 2006). Thus, methylation of R234 might affect the spatial organization of residues that do directly interact with the coenzyme in the catalytic pocket. Modification-resistant and mimicry mutants

are important tools for studies of post-translational modification (Lin et al., 2013; Xiong and Guan, 2012). Methyl groups on arginine residues increase their stereo hindrance without completely neutralizing the residue's positive charge (Paik et al., 2007). Thus, arginine-to-lysine and arginine-to-phenylalanine mutations are used to mimic unmethylated and methylated states, respectively. However, the R234K mutation unexpectedly inactivated GAPDH. This finding suggests that R234, which is located in the catalytic pocket, is required for the catalytic activity of GAPDH. The R234K mutant is unable to totally mimic unmethylated GAPDH.

Previous studies have reported that CARM1 is overexpressed and acts as an oncogenic protein in several different cancer types (Yang and Bedford, 2013). However, recent studies indicate that CARM1 also functions as a tumor suppressor protein in pancreatic and lung cancer (Wang et al., 2016; O'Brien et al., 2010). These observations suggest that the function of CARM1 in cancer is context-dependent. Here we find that CARM1 expression is decreased in malignant liver cancer, indicative of a tumor suppressor role. Large-scale cohort studies and detailed immunohistochemical analysis of CARM1 in cancer samples would be invaluable to better understand the role CARM1 plays in liver cancer progression. The prognostic value of CARM1 expression and subcellular localization also merits future investigation.

Protein arginine methylation is emerging as a key regulatory mechanism of cellular metabolism. Glucose is repurposed for the pentose phosphate pathway when fructose-2,6-bisphosphatase 3 (PFKFB3) is hypomethylated to cope with oxidative stress (Yamamoto et al., 2014). Glutamine metabolism is also modulated by arginine methylation of malate dehydrogenase 1 (MDH1) in pancreatic cancer (Wang et al., 2016). Upon exposure to the glucose-rich environment, cancer cells turn on their metabolic machinery to utilize more carbon sources. From our findings, we propose that AMPK senses cellular glucose levels and suppresses the expression of CARM1 when glucose levels are high. The consequent hypomethylation of R234 activates GAPDH to promote glycolysis, which further increases the growth of liver cancer cells (Figure 7F). Thus, small molecules that function as CARM1 activators might have therapeutic potential for suppressing GAPDH and liver cancer growth. Collectively, our study demonstrates that CARM1-mediated GAPDH methylation plays a key role in coordinating cancer metabolism and nutrient sensing.

(D). R234 methylation and the enzymatic activity of immunopurified WT and mutant GAPDH were determined by western blot and spectrofluorometer, respectively. Relative enzymatic activity was presented as mean  $\pm$  SD of triplicate experiments and was statistically analyzed using unpaired Student's t test. (E and F) R234 methylation of GAPDH modulates the level of glycolytic intermediates. GAPDH knockdown HepG2 cells re-expressing WT GAPDH or its R234F mutant were treated with TP-064 (E) or transduced with a virus carrying CARM1 shRNA (F). Glycolytic intermediates were extracted and determined by liquid chromatography-tandem mass spectrometry (LC-MS/MS). Relative metabolites abundance was presented as mean  $\pm$  SD of triplicate experiments and was statistically analyzed using unpaired Student's t test. \* $p < 0.05$ .

(G and H) R234 methylation of GAPDH decreases the extracellular acidification rate (ECAR) of HepG2 cells. GAPDH knockdown HepG2 cells re-expressing WT GAPDH or its R234F mutant were treated with TP-064 (G) or transduced with a virus carrying CARM1 shRNA (H). The ECAR was measured in an XF96 extracellular analyzer. Each data point represents triplicate experiments with mean  $\pm$  SD, which was statistically analyzed using unpaired Student's t test. \*\* $p < 0.01$ , \* $p < 0.05$ .

(I and J) R234 methylation of GAPDH mildly decreases the basal oxygen consumption rate (OCR) of HepG2 cells. CARM1 was inhibited by TP-064 (I) or depleted by shRNA (J) in GAPDH knockdown HepG2 cells re-expressing WT GAPDH or its R234F mutant. OCR was measured in an XF96 extracellular analyzer. Each data point represents triplicate experiments with mean  $\pm$  SD, which was statistically analyzed using unpaired Student's t test. \* $p < 0.05$ .

\*\* $p < 0.01$ . See also Figure S4.

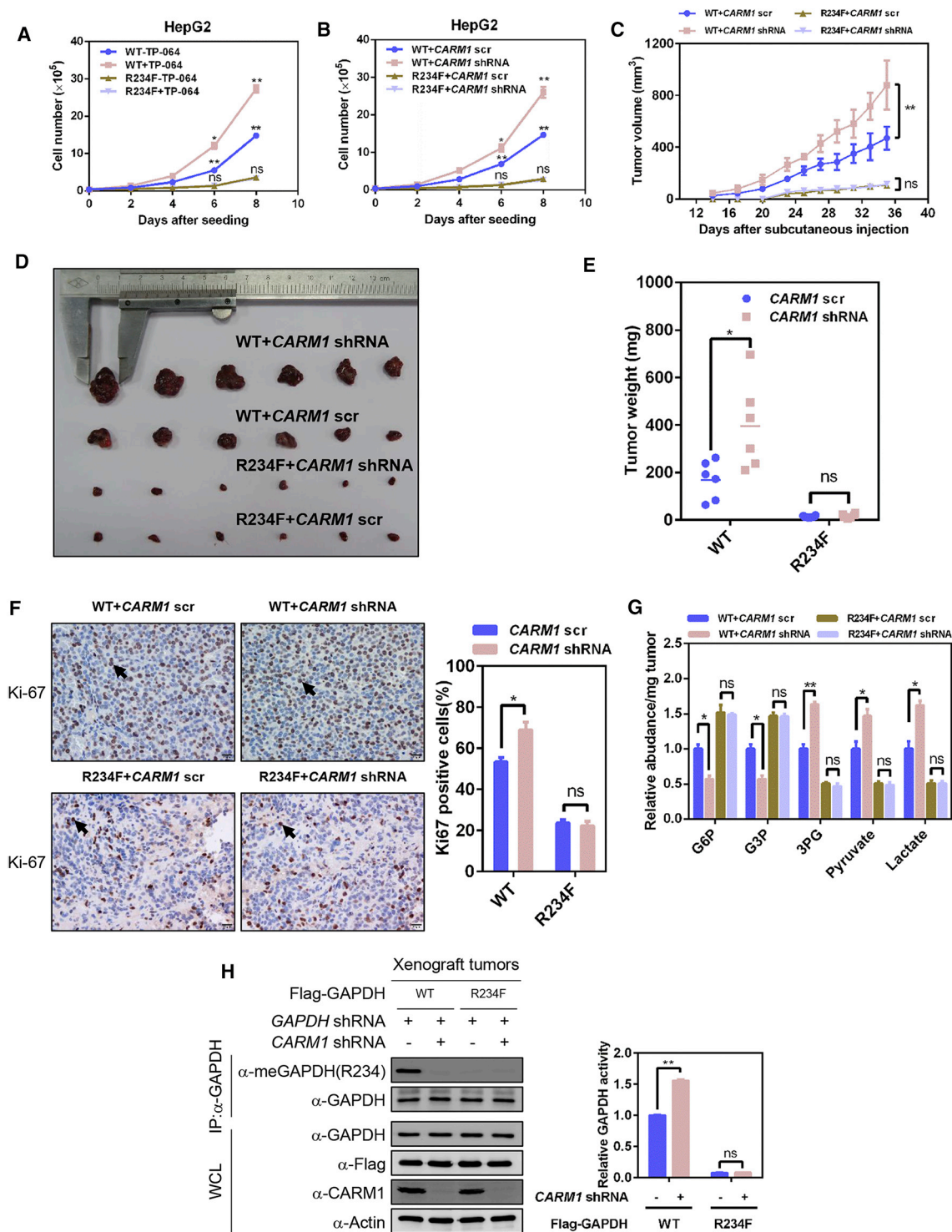


**Figure 6. GAPDH R234 Methylation Delays Liver Cancer Cell Growth**

(A and B) R234 methylation of GAPDH suppresses the proliferation of HepG2 cells. CARM1 was suppressed by TP-064 (A) or knocked down by shRNA (B) in GAPDH knockdown HepG2 cells re-expressing WT GAPDH or its R234F mutant. Cell proliferation was determined. Each data point was presented as mean  $\pm$  SD of triplicate experiments and was statistically analyzed using unpaired Student's t test. \*\* $p < 0.01$ , \* $p < 0.05$ . Scr, scramble shRNA.

(C–E) R234 methylation of GAPDH delays the tumor growth of liver cancer cells in a xenograft model. WT GAPDH and its R234F mutant were stably expressed in GAPDH/CARM1 double knockdown HepG2 cells. The growth of xenografts was monitored over 5 weeks (C). Xenograft tumors were then dissected and their

(legend continued on next page)

## EXPERIMENTAL PROCEDURES

### Plasmids

The cDNA encoding full-length human GAPDH was cloned into the FLAG-tagged vector pcDNA3.1 and the His-tagged vector pSJ3. Plasmids encoding PRMTs were obtained from Dr. Yanzhong Yang (City of Hope National Medical Center, Los Angeles, USA). Point mutations of GAPDH and CARM1 were generated by site-directed mutagenesis using a QuikChange Site-Directed Mutagenesis Kit (Stratagene). FLAG-tagged WT GAPDH or its R234K and R234F mutants were subcloned into pQCXIH. shRNA oligos were synthesized and annealed and cloned into pMKO.1 or pBasi-hU6-Neo. All expression constructs were verified by DNA sequencing.

### Antibodies

Antibodies against FLAG (Cell Signaling Technology, catalog number 2368), GAPDH (Proteintech, catalog number 10494-1-AP), CARM1 (Cell Signaling Technology, catalog number 12495), AMPK $\alpha$  (Cell Signaling Technology, catalog number 2532), phospho-AMPK $\alpha$  (Cell Signaling Technology, catalog number 2535), actin (AOGMA, catalog number 9601), GFP (Proteintech, catalog number 66002-1-Ig), phospho-Ser/Thr (Cell Signaling Technology, catalog number 9631), LC3B (Cell Signaling Technology, catalog number 2775), monomethyl arginine (Cell Signaling Technology, catalog number 8015S), symmetric dimethylarginine (Cell Signaling Technology, catalog number 13222), and asymmetrical dimethylarginine (Cell Signaling Technology, catalog number 13522) were purchased commercially. To generate a site-specific antibody to detect the asymmetric di-methyl R234 of GAPDH ( $\alpha$ -meGAPDH(R248)), the synthesized peptide TGMAFR(me2a)VPTANVC (GL Biochem) was coupled to keyhole limpet hemocyanin (KLH) as an antigen to immunize rabbits. Anti-serum was collected after five doses of immunization.

### Cell Culture and Treatment

The cells used in this study were cultured in DMEM (Gibco, catalog number 12100046) supplemented with 10% fetal bovine serum (FBS) (Gibco, catalog number 0082147) and 1% penicillin and streptomycin (HyClone, catalog number SV30010). For PRMT inhibitor treatment, 40  $\mu$ M AdOx (Sigma, catalog number A7154), 20  $\mu$ M AML-1 (Selleck, catalog number S7884), or 10  $\mu$ M TP-064 (Tocris, catalog number 6008) was added to the culture medium when the cells were 50% to 60% confluent. After 24 hr of AdOx and AML-1 treatment or after 12 hr of TP-064 treatment, cells were harvested for further analysis. For glucose starvation, DMEM-containing glucose was aspirated, cells were washed twice with PBS, and glucose-free DMEM (Gibco, catalog number 11966025) was added. For MG132 treatment, 10  $\mu$ M MG132 was added to the culture medium 6 hr before cells were harvested.

### Immunoprecipitation and Western Blotting

Cells were lysed in NP-40 lysis buffer (150 mM NaCl, 50 mM Tris, and 0.3% NP-40 [pH 7.5]) with protease inhibitors (Biotool, catalog number B14001) at 4°C for 1 hr. For exogenous IP and co-immunoprecipitation (coIP), FLAG beads (Sigma, catalog number A2220) were added to the cell lysates and incubated at 4°C for 4 hr. The beads were then washed three times with NP-40 lysis

buffer and used for further analysis. For endogenous IP and coIP, antibodies against GAPDH or CARM1 were added to cell lysates and incubated at 4°C overnight. Then protein G beads (Roche) were added to the cell lysates and incubated at 4°C for another 4 hr. Standard western blotting protocols were used to analyze the results of the IP and coIP experiments.

### Determination of GAPDH Activity

To assay GAPDH enzymatic activity, reactions were conducted in 1 mL mixture containing 896  $\mu$ L pyrophosphate and arsenate buffer (0.015 M Na<sub>4</sub>P<sub>2</sub>O<sub>7</sub> and 0.03 M Na<sub>2</sub>HASO<sub>4</sub> [pH 8.5]), 33  $\mu$ L NAD<sup>+</sup> (7.5 mM), 33  $\mu$ L G3P (7.5 mM), 33  $\mu$ L DTT (100 mM), and 5  $\mu$ L purified GAPDH protein at 37°C. Enzyme activity was monitored as an absorbance increase at 340 nm using a spectrofluorometer (FL-4600, Hitachi). Three independent experiments were performed. To determine K<sub>m</sub>, serial concentrations of NAD<sup>+</sup> or G3P at 0.00, 24.75, 49.50, 165.00, 247.50, 412.50, 495.00, and 750.00  $\mu$ M were used to measure the enzymatic activity of GAPDH. The K<sub>m</sub> value was determined using the Michaelis-Menten curve plotted by GraphPad Prism.

### Recombinant Protein Expression and Purification

Plasmids encoding recombinant GAPDH and CARM1 were transformed into the BL21 strain, and bacterial culture was induced with isopropyl  $\beta$ -D-1-thiogalactopyranoside (IPTG) at 16°C for 12 hr when the optical density 600 (OD<sub>600</sub>) reached 0.6. BL21 cells were lysed by ultrasonication and purified with GST agarose beads (AOGMA, catalog number AGM90049) for glutathione S-transferase (GST)-CARM1 or with nickel-nitrilotriacetic acid (Ni-NTA) agarose beads (Sigma, catalog number P6611) for His-GAPDH.

### In Vitro Methylation Assay

The *in vitro* methylation reaction was performed in 30  $\mu$ L PBS containing 3  $\mu$ g His-GAPDH, 3  $\mu$ g CARM1, and 3  $\mu$ M S-adenosyl methionine (SAM) (Sigma, A4377). Methylation reactions were initiated by the addition of purified CARM1 and incubated at 30°C for 1.5 hr. After *in vitro* methylation, R234 methylation and GAPDH activity were determined.

### Real-Time qPCR Analysis

Total RNA was extracted from HepG2, Huh7, MEF, and 293A cells using TRNzol Universal reagent (Tiangen, catalog number DP424). 2  $\mu$ g of total RNA was reverse-transcribed according to the manufacturer's instructions (Takara, catalog number RR047B). qPCR was conducted with SYBR Green Premix reagent (Takara, catalog number RR820A) using the following primers:

*mActb* forward primer: 5'-GGCTGTATCCCTCCATCG-3',  
*mActb* reverse primer: 5'-CCAGTTGGTAAACAATGCCATGT-3',  
*mCarm1* forward primer: 5'-CAGGCTCCAAGTCCAGTAACC-3',  
*mCarm1* reverse primer: 5'-GGGAGTGGGTGTGATTGACA-3',  
*hACTB* forward primer: 5'-GCCGACAGGATGCAGAAGGAGATCA-3',  
*hACTB* reverse primer: 5'-AAGCATTTCGGTGGACGATGGA-3',  
*hCARM1* forward primer: 5'-CTGGCTTCTGGTTTGACG-3',  
*hCARM1* reverse primer: 5'-CAGGAGGTTACTGGACTTGGA-3'.

Relative gene expression was calculated using the comparative C(T) method based on three independent experiments.

weights determined (D and E). Each data point was presented as mean  $\pm$  SD of triplicate experiments and was statistically analyzed using unpaired Student's t test. \*\*p < 0.01, \*p < 0.05.

(F) R234 methylation decreases Ki-67 staining in tumor xenograft samples. Immunohistochemistry (IHC) was performed using the  $\alpha$ -Ki67 antibody and hematoxylin. Ki-67-positive cells, denoted by arrows, were quantified and analyzed (right). Percentage of Ki67 positive cell is presented as mean  $\pm$  SD calculated from three different view and was statistically analyzed using unpaired Student's t test. \*p < 0.05.

(G) R234 methylation of GAPDH modulates the level of glycolytic metabolites in tumor xenografts. Metabolites were extracted from the tumor and detected by LC-MS/MS. Relative abundance value was presented as mean  $\pm$  SD calculated from three xenograft samples and was statistically analyzed using unpaired Student's t test. \*p < 0.05.

(H) R234 methylation and enzymatic activity of GAPDH in tumor xenografts were determined by western blot and spectrofluorometer, respectively. Xenograft tumors were homogenized, and GAPDH was immunopurified. The stable knockdown efficiency and sustained expression of FLAG-tagged GAPDH in xenograft tissue were validated by western blot. Relative GAPDH enzyme activity was presented as mean  $\pm$  SD calculated from three xenograft samples and was statistically analyzed using unpaired Student's t test.

\*\*p < 0.01. See also Figure S5.

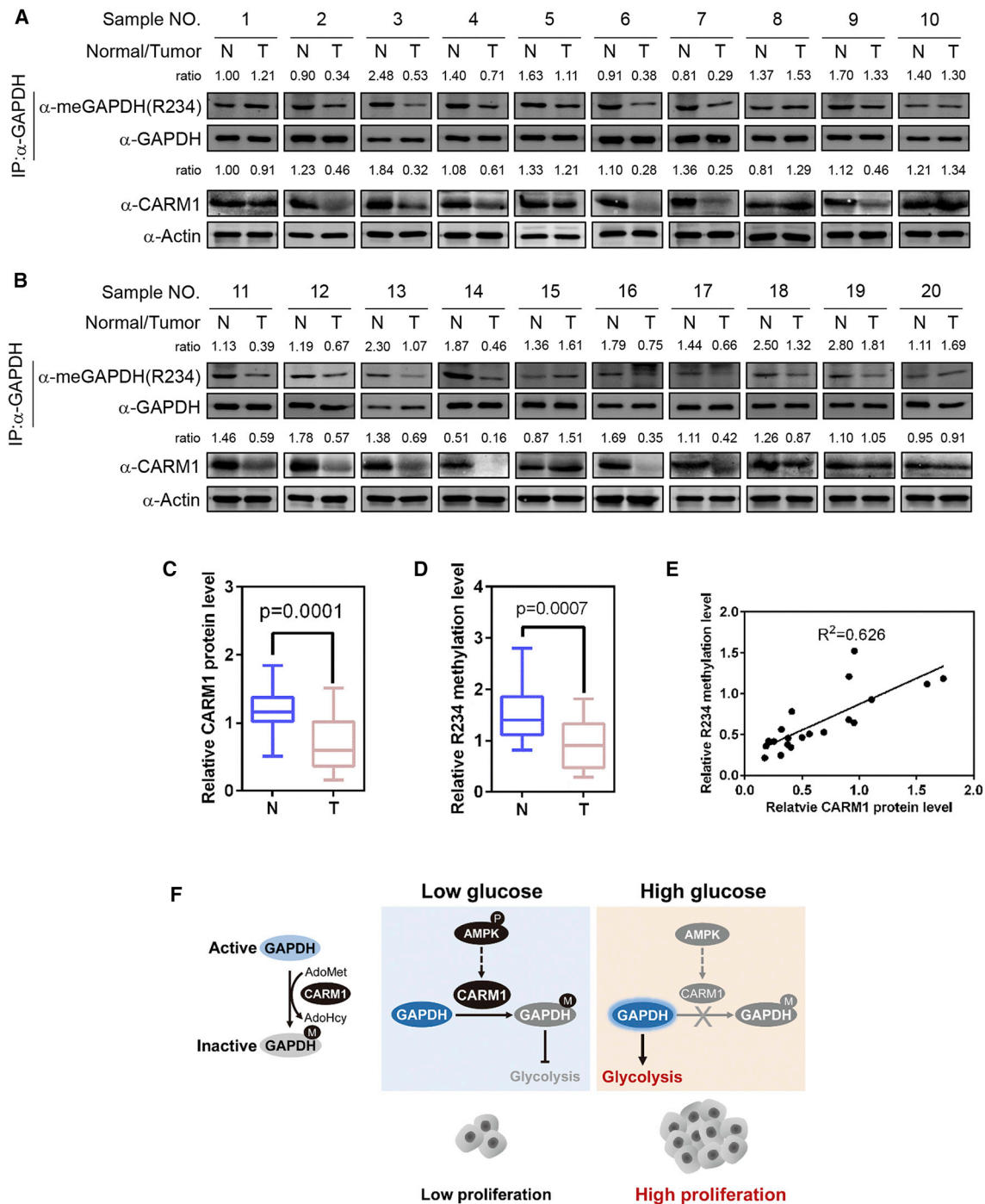


**Figure 7. GAPDH R234 Is Hypomethylated in Human Hepatocellular Carcinoma**

(A–D) CARM1 protein levels and the R234 methylation of GAPDH immunoprecipitated from human hepatocellular carcinoma (HCC) patient samples were determined by immunoblotting in both tumor (T) and adjacent normal tissue (N) (A and B). CARM1 protein (C) and R234 methylation (D) levels in normal and cancerous tissues were statistically analyzed. Relative CARM1 protein level and R234 methylation level was presented as mean  $\pm$  SD calculated from twenty HCC samples and was statistically analyzed by paired Student's t test.

(E) CARM1 protein and R234 methylation levels are positively correlated in HCC patient samples.

(F) Working model for CARM1-induced methylation of GAPDH. M, methylation; P, phosphorylation. The dashed line between AMPK and CARM1 indicates that AMPK regulates the CARM1 protein level indirectly.

### Construction of Stable Cell Pools and Cell Proliferation Assay

To generate stable *CARM1* knockdown or *GAPDH* knockdown or *GAPDH/CARM1* double knockdown cell pools, shRNAs targeting *CARM1* or *GAPDH* were constructed. Targeting sequences are as follows:

sh*GAPDH*-#1: 5'-CCCTTCATTGACCTCAACT-3',  
sh*CARM1*-#1: 5'-GCAAGCAGTCCTTCATCATCACTC-3',  
sh*CARM1*-#2: 5'-GGACAAGATCGTTCTTGATGTCTC-3'.

Retroviruses were produced by using a two-plasmid packaging system. Cells were infected with the retrovirus and selected in 0.8  $\mu\text{g}/\text{mL}$  puromycin (AMERESCO, catalog number J593) or in 200  $\mu\text{g}/\text{mL}$  G418 (Selleck, catalog number S3028) for 1 week. To generate *GAPDH* knockdown or *GAPDH/CARM1* double knockdown and to rescue stable cell pools, FLAG-tagged human WT *GAPDH* or its R234F mutant were cloned into the retroviral pQCXIH vector and co-transfected with vectors expressing the gag and vsvg genes in HEK293T cells to produce retroviruses. Cells with stable *GAPDH* knockdown or *GAPDH/CARM1*-double knockdown were then infected with the WT *GAPDH* or R234F mutant-expressing retroviruses, followed by selection in 50  $\mu\text{g}/\text{mL}$  hygromycin B (AMERESCO, catalog number K547) for 1 week. For the cell proliferation assay,  $1 \times 10^4$  Huh7 cells or  $4 \times 10^4$  HepG2 cells were seeded in triplicates in six-well plates. Cell numbers were counted every 48 hr for 8 days using a hemocytometer (Brand, catalog number 717805).

### Glucose and Lactate Detection

$1 \times 10^6$  cells were seeded in six-well plates. The culture medium was then collected 12 hr after being replaced and filtered using a 10-kD spin column (Abcam, catalog number ab93349). Glucose and lactate were determined using a glucose assay kit (Sigma, catalog number GAGO20) and a lactate assay kit (Sigma, catalog number MAK064), respectively. Glucose uptake was determined by subtracting the final medium glucose concentration from the initial medium glucose concentration in the culture medium. Data were obtained from three independent triplicates and normalized against cell number.

### Metabolites Extraction

$1 \times 10^7$  cells were re-suspended in 1 mL of ice-cold 80% methanol and 20% sterile ultra-pure water ( $\text{ddH}_2\text{O}$ ). Samples were vigorously vortexed and placed in liquid  $\text{N}_2$  for 10 min to freeze and in ice for 10 min to thaw. The freeze-thaw cycle was repeated four times. Samples were centrifuged at 13,000 rpm for 15 min to pellet cell debris, lipids, and proteins. The supernatant was evaporated, and the resulting metabolites were re-suspended in 10% methanol and 90% high performance liquid chromatography (HPLC)-grade  $\text{H}_2\text{O}$ .

### Metabolite Analysis by Liquid Chromatography-Tandem Mass Spectrometry

The metabolites samples were re-suspended in 80  $\mu\text{L}$  10% methanol and 90% HPLC-grade  $\text{H}_2\text{O}$  for mass spectrometry. 20  $\mu\text{L}$  of each sample was injected and analyzed using a 6500 Q-Trap triple quadrupole mass spectrometer (AB Sciex) coupled to a Prominence HPLC system (Shimadzu) via multiple reaction monitoring (MRM). Metabolites were targeted in negative ion mode (IonSpray voltage:  $-4,500$  V). An Ultimate AQ-C18 column (1.7  $\mu\text{m}$ ,  $2.1 \times 250$  mm, Welch) was used to separate G6P, G3P, 3-PG, pyruvate, and lactate. Monitored transitions were as follows: G6P, mass-to-charge ratio (*m/z*) 259 > 97 (collision energy, [CE],  $-18$  V); G3P, *m/z* 169 > 79 (CE:  $-20$  V); 3-PG, *m/z* 185 > 79 (CE,  $-44$  V); pyruvate, *m/z* 87.0 > 43.0 (CE,  $-10$  V); lactate, *m/z* 89.0 > 43.0 (CE,  $-13$  V). Peak areas from the total ion current for each metabolite were integrated using Skyline software (AB Sciex).

### Measurement of ECAR and OCR

The ECAR and OCR were measured in an XF96 extracellular analyzer (Seahorse Bioscience). A total of  $2 \times 10^4$  cells per well were seeded into a 96-well plate and incubated in DMEM with 10% FBS at  $37^\circ\text{C}$ . The next day, the medium was changed to XF base medium containing 2 mM glutamine for ECAR measurement or containing 10 mM glucose, 2 mM glutamine, and 1 mM sodium pyruvate for OCR measurement. The cells were incubated in a  $\text{CO}_2$ -free incubator at  $37^\circ\text{C}$  for 1 h before measurement. For ECAR detection,

cells were sequentially exposed to 10 mM glucose, 2  $\mu\text{M}$  oligomycin, and 50 mM 2-deoxyglucose (2-DG). For OCR determination, cells were sequentially exposed to 2  $\mu\text{M}$  oligomycin, 1  $\mu\text{M}$  carbonyl cyanide-4-(trifluoromethoxy)phenylhydrazone (FCCP), and 0.5  $\mu\text{M}$  rotenone and antimycin A. Each point in the traces represents the average measurement from triplicate experiments.

### Xenograft Studies

All animal procedures were performed in accordance with the approval of the animal care committee at Fudan University. *GAPDH/CARM1* double knockdown HepG2 cells re-expressing WT *GAPDH* or the R234F mutant were trypsinized and re-suspended in a mixture of 50% PBS and 50% Matrigel (Corning, catalog number 354248). BALB/c-nude mice (nu/nu, male, 4 weeks old) were purchased from Shanghai Sippr-BK Laboratory Animal Company (Shanghai). Mice were injected subcutaneously with  $5 \times 10^6$  cells ( $n = 6$  for each group). Two weeks later, the major and minor diameter of tumors were measured every 2 days, and tumors were harvested 5 weeks after injection. Tumor volume was calculated using the formula of  $1/2 \times \text{major diameter} \times \text{minor diameter}^2$ .

### Ki67 Staining

Xenograft sections were deparaffinized in xylene and hydrated in graded ethanol, followed by deionized water. Endogenous peroxidase activity was inactivated with 3% hydrogen peroxidase in methanol for 30 min. Antigen retrieval was performed by boiling the sections in 0.01 M citrate buffer (pH 6.0) for 25 min in a microwave oven. The sections were incubated with normal goat serum for 20 min to block non-specific staining and then incubated overnight at  $4^\circ\text{C}$  with the Ki67 antibody (Abcam, catalog number ab15580) at 1:200 dilution. After incubation for 45 min with a horseradish peroxidase (HRP)-conjugated anti-rabbit secondary antibody, the sections were stained using a diaminobenzidine (DAB) kit according to the manufacturer's instructions (Long Island Antibody, catalog number DAB-50T), followed by counterstaining with hematoxylin.

### HCC Samples

Hepatocellular carcinoma patient samples were obtained from Tongji University Affiliated 10th People's Hospital, Shanghai, with written consent from all patients. Procedures related to human subjects were approved by the Ethics Committee of the Institutes of Biomedical Sciences, Fudan University. The *CARM1* protein level and arginine methylation level of immunopurified *GAPDH* were determined using western blot with  $\alpha$ -*CARM1* and  $\alpha$ -*meGAPDH*(R234) antibodies.

### Statistical Analysis

Statistical analyses were performed with a two-tailed unpaired Student's *t* test. All data shown represent the results obtained from triplicate independent experiments with SEM (mean  $\pm$  SD). ns, not significant, \* $p < 0.05$ , \*\* $p < 0.01$ , \*\*\* $p < 0.001$ .

### DATA AND SOFTWARE AVAILABILITY

The accession number for the raw data reported in this paper is Mendeley: <https://doi.org/10.17632/xf82gjbxb.1>.

### SUPPLEMENTAL INFORMATION

Supplemental Information includes five figures and can be found with this article online at <https://doi.org/10.1016/j.celrep.2018.08.066>.

### ACKNOWLEDGMENTS

We thank the members of the Cancer Metabolism Laboratory for discussions and support throughout this study. We thank Dr. Yanzhong Yang (City of Hope) for sharing plasmids encoding PRMTs and Hongyu Gu (Shanghai Cancer Institute, Fudan University) for support with the IHC. We also thank the Biomedical Core Facility, Fudan University for technical support. This study is funded by

MOST grant 2015CB910401 (to Q.-Y.L.), the Natural Science Foundation of China (81790253, and 81430057 to Q.-Y.L. and 81772946 to Y.-P.W.), and the Innovation Program of Shanghai Municipal Education Commission (N173606 to Q.-Y.L.).

#### AUTHOR CONTRIBUTIONS

X.-Y.Z. and X.-M.Y. performed experiments and analyzed the data. Y.-Y.X., M.Y., and W.-W.Y. contributed to the enzymatic activity measurements. L.-M.W. and H.-J.L. assisted with the IEF experiments. S.-W.Z. provided and characterized HHC samples. Y.-P.W. and Q.-Y.L. conceived and supervised the project. X.-Y.Z., Y.-P.W., and Q.-Y.L. co-wrote the manuscript.

#### DECLARATION OF INTERESTS

The authors declare no competing interests.

Received: January 15, 2018

Revised: May 3, 2018

Accepted: August 22, 2018

Published: September 18, 2018

#### REFERENCES

- Al-Dhaheeri, M., Wu, J., Skliris, G.P., Li, J., Higashimoto, K., Wang, Y., White, K.P., Lambert, P., Zhu, Y., Murphy, L., and Xu, W. (2011). CARM1 is an important determinant of ER $\alpha$ -dependent breast cancer cell differentiation and proliferation in breast cancer cells. *Cancer Res.* **71**, 2118–2128.
- Bedford, M.T., and Clarke, S.G. (2009). Protein arginine methylation in mammals: who, what, and why. *Mol. Cell* **33**, 1–13.
- Chang, C., Su, H., Zhang, D., Wang, Y., Shen, Q., Liu, B., Huang, R., Zhou, T., Peng, C., Wong, C.C., et al. (2015). AMPK-Dependent Phosphorylation of GAPDH Triggers Sirt1 Activation and Is Necessary for Autophagy upon Glucose Starvation. *Mol. Cell* **60**, 930–940.
- Cheung, N., Chan, L.C., Thompson, A., Cleary, M.L., and So, C.W. (2007). Protein arginine-methyltransferase-dependent oncogenesis. *Nat. Cell Biol.* **9**, 1208–1215.
- Dang, C.V. (2012). Links between metabolism and cancer. *Genes Dev.* **26**, 877–890.
- Frietze, S., Lupien, M., Silver, P.A., and Brown, M. (2008). CARM1 regulates estrogen-stimulated breast cancer growth through up-regulation of E2F1. *Cancer Res.* **68**, 301–306.
- Gao, W.W., Xiao, R.Q., Peng, B.L., Xu, H.T., Shen, H.F., Huang, M.F., Shi, T.T., Yi, J., Zhang, W.J., Wu, X.N., et al. (2015). Arginine methylation of HSP70 regulates retinoid acid-mediated *RAR* $\beta$ 2 gene activation. *Proc. Natl. Acad. Sci. USA* **112**, E3327–E3336.
- Garcia, D., and Shaw, R.J. (2017). AMPK: Mechanisms of Cellular Energy Sensing and Restoration of Metabolic Balance. *Mol. Cell* **66**, 789–800.
- Gu, H., Ren, J.M., Jia, X., Levy, T., Rikova, K., Yang, V., Lee, K.A., Stokes, M.P., and Silva, J.C. (2016). Quantitative Profiling of Post-translational Modifications by Immunoaffinity Enrichment and LC-MS/MS in Cancer Serum without Immunodepletion. *Mol. Cell. Proteomics* **15**, 692–702.
- Guo, A., Gu, H., Zhou, J., Mulhern, D., Wang, Y., Lee, K.A., Yang, V., Aguiar, M., Kornhauser, J., Jia, X., et al. (2014). Immunoaffinity enrichment and mass spectrometry analysis of protein methylation. *Mol. Cell. Proteomics* **13**, 372–387.
- Hanahan, D., and Weinberg, R.A. (2011). Hallmarks of cancer: the next generation. *Cell* **144**, 646–674.
- Hardie, D.G. (2014). AMPK—sensing energy while talking to other signaling pathways. *Cell Metab.* **20**, 939–952.
- Hsu, J.-M., Chen, C.-T., Chou, C.-K., Kuo, H.-P., Li, L.-Y., Lin, C.-Y., Lee, H.-J., Wang, Y.-N., Liu, M., Liao, H.-W., et al. (2011). Crosstalk between Arg 1175 methylation and Tyr 1173 phosphorylation negatively modulates EGFR-mediated ERK activation. *Nat. Cell Biol.* **13**, 174–181.
- Ismail, S.A., and Park, H.W. (2005). Structural analysis of human liver glyceraldehyde-3-phosphate dehydrogenase. *Acta Crystallogr. D Biol. Crystallogr.* **61**, 1508–1513.
- Jenkins, J.L., and Tanner, J.J. (2006). High-resolution structure of human D-glyceraldehyde-3-phosphate dehydrogenase. *Acta Crystallogr. D Biol. Crystallogr.* **62**, 290–301.
- Kuzminskaya, E.V., Asryants, R.A., and Nagradova, N.K. (1991). Rabbit muscle tetrameric D-glyceraldehyde-3-phosphate dehydrogenase is locked in the asymmetric state by chemical modification of a single arginine per subunit. *Biochim. Biophys. Acta* **1075**, 123–130.
- Larsen, S.C., Sylvestersen, K.B., Mund, A., Lyon, D., Mullari, M., Madsen, M.V., Daniel, J.A., Jensen, L.J., and Nielsen, M.L. (2016). Proteome-wide analysis of arginine monomethylation reveals widespread occurrence in human cells. *Sci. Signal.* **9**, rs9.
- Lash, A.E., Tolstoshev, C.M., Wagner, L., Schuler, G.D., Strausberg, R.L., Riggin, G.J., and Altschul, S.F. (2000). SAGEmap: a public gene expression resource. *Genome Res.* **10**, 1051–1060.
- Lehninger, A.L., Nelson, D.L., and Cox, M.M. (2013). *Lehninger principles of biochemistry* (W.H. Freeman), p. 535.
- Li, T., Liu, M., Feng, X., Wang, Z., Das, I., Xu, Y., Zhou, X., Sun, Y., Guan, K.-L., Xiong, Y., and Lei, Q.Y. (2014). Glyceraldehyde-3-phosphate dehydrogenase is activated by lysine 254 acetylation in response to glucose signal. *J. Biol. Chem.* **289**, 3775–3785.
- Liao, H.-W., Hsu, J.-M., Xia, W., Wang, H.-L., Wang, Y.-N., Chang, W.-C., Arold, S.T., Chou, C.-K., Tsou, P.-H., Yamaguchi, H., et al. (2015). PRMT1-mediated methylation of the EGF receptor regulates signaling and cetuximab response. *J. Clin. Invest.* **125**, 4529–4543.
- Lin, R., Tao, R., Gao, X., Li, T., Zhou, X., Guan, K.L., Xiong, Y., and Lei, Q.Y. (2013). Acetylation stabilizes ATP-citrate lyase to promote lipid biosynthesis and tumor growth. *Mol. Cell* **51**, 506–518.
- Liu, F., Ma, F., Wang, Y., Hao, L., Zeng, H., Jia, C., Wang, Y., Liu, P., Ong, I.M., Li, B., et al. (2017a). PKM2 methylation by CARM1 activates aerobic glycolysis to promote tumorigenesis. *Nat. Cell Biol.* **19**, 1358–1370.
- Liu, S., Sun, Y., Jiang, M., Li, Y., Tian, Y., Xue, W., Ding, N., Sun, Y., Cheng, C., Li, J., et al. (2017b). Glyceraldehyde-3-phosphate dehydrogenase promotes liver tumorigenesis by modulating phosphoglycerate dehydrogenase. *Hepatology* **66**, 631–645.
- O'Brien, K.B., Alberich-Jordà, M., Yadav, N., Kocher, O., Diruscio, A., Ebralidze, A., Levantini, E., Sng, N.J., Bhasin, M., Caron, T., et al. (2010). CARM1 is required for proper control of proliferation and differentiation of pulmonary epithelial cells. *Development* **137**, 2147–2156.
- Onwuli, D.O., Rigau-Roca, L., Cawthorne, C., and Beltran-Alvarez, P. (2017). Mapping arginine methylation in the human body and cardiac disease. *Proteomics Clin. Appl.* **11**, 1–9.
- Paik, W.K., Paik, D.C., and Kim, S. (2007). Historical review: the field of protein methylation. *Trends Biochem. Sci.* **32**, 146–152.
- Poornima, G., Shah, S., Vignesh, V., Parker, R., and Rajyaguru, P.I. (2016). Arginine methylation promotes translation repression activity of eIF4G-binding protein, Scd6. *Nucleic Acids Res.* **44**, 9358–9368.
- Ripple, M.O., and Wilding, G. (1995). Alteration of glyceraldehyde-3-phosphate dehydrogenase activity and messenger RNA content by androgen in human prostate carcinoma cells. *Cancer Res.* **55**, 4234–4236.
- Schek, N., Hall, B.L., and Finn, O.J. (1988). Increased glyceraldehyde-3-phosphate dehydrogenase gene expression in human pancreatic adenocarcinoma. *Cancer Res.* **48**, 6354–6359.
- Shia, W.J., Okumura, A.J., Yan, M., Sarkeshik, A., Lo, M.C., Matsuura, S., Komeno, Y., Zhao, X., Nimer, S.D., Yates, J.R., 3rd, and Zhang, D.E. (2012). PRMT1 interacts with AML1-ETO to promote its transcriptional activation and progenitor cell proliferative potential. *Blood* **119**, 4953–4962.
- Shin, H.-J.R., Kim, H., Oh, S., Lee, J.-G., Kee, M., Ko, H.-J., Kweon, M.-N., Won, K.-J., and Baek, S.H. (2016). AMPK-SKP2-CARM1 signalling cascade in transcriptional regulation of autophagy. *Nature* **534**, 553–557.

- Strausberg, R.L., Greenhut, S.F., Grouse, L.H., Schaefer, C.F., and Buetow, K.H. (2001). *In silico* analysis of cancer through the Cancer Genome Anatomy Project. *Trends Cell Biol.* *11*, S66–S71.
- Tokunaga, K., Nakamura, Y., Sakata, K., Fujimori, K., Ohkubo, M., Sawada, K., and Sakiyama, S. (1987). Enhanced expression of a glyceraldehyde-3-phosphate dehydrogenase gene in human lung cancers. *Cancer Res.* *47*, 5616–5619.
- Walport, L.J., Hopkinson, R.J., Chowdhury, R., Schiller, R., Ge, W., Kawamura, A., and Schofield, C.J. (2016). Arginine demethylation is catalysed by a subset of JmjC histone lysine demethylases. *Nat. Commun.* *7*, 11974–11986.
- Wang, Y.P., Zhou, W., Wang, J., Huang, X., Zuo, Y., Wang, T.S., Gao, X., Xu, Y.Y., Zou, S.W., Liu, Y.B., et al. (2016). Arginine Methylation of MDH1 by CARM1 Inhibits Glutamine Metabolism and Suppresses Pancreatic Cancer. *Mol. Cell* *64*, 673–687.
- Warburg, O. (1956). On the origin of cancer cells. *Science* *123*, 309–314.
- Xiong, Y., and Guan, K.L. (2012). Mechanistic insights into the regulation of metabolic enzymes by acetylation. *J. Cell Biol.* *198*, 155–164.
- Yamamoto, T., Takano, N., Ishiwata, K., Ohmura, M., Nagahata, Y., Matsuura, T., Kamata, A., Sakamoto, K., Nakanishi, T., Kubo, A., et al. (2014). Reduced methylation of PFKFB3 in cancer cells shunts glucose towards the pentose phosphate pathway. *Nat. Commun.* *5*, 3480.
- Yang, Y., and Bedford, M.T. (2013). Protein arginine methyltransferases and cancer. *Nat. Rev. Cancer* *13*, 37–50.
- Yang, Y., Hadjikyriacou, A., Xia, Z., Gayatri, S., Kim, D., Zurita-Lopez, C., Kelly, R., Guo, A., Li, W., Clarke, S.G., and Bedford, M.T. (2015). PRMT9 is a type II methyltransferase that methylates the splicing factor SAP145. *Nat. Commun.* *6*, 6428–6440.
- Zhao, D.Y., Gish, G., Braunschweig, U., Li, Y., Ni, Z., Schmitges, F.W., Zhong, G., Liu, K., Li, W., Moffat, J., et al. (2016). SMN and symmetric arginine dimethylation of RNA polymerase II C-terminal domain control termination. *Nature* *529*, 48–53.